Technical Report RT-136

Simplified bidimensional water temperature modelling during spring time on the St. Lawrence River

Jean Morin, Olivier Champoux and Yves Secretan

March 2004

For reference:

Morin, J., O. Champoux and Y. Secretan (2004). Simplified bidimensional water temperature modelling during spring time on the St. Lawrence River. Technical Report MSC Québec – Hydrology RT-136, Environment Canada, Sainte-Foy, prepared for the Environmental Technical Working Group (ETWG) of the International Lake Ontario – St. Lawrence River Study Board (International Joint Commission). 39 pages.

RESEARCH TEAM

Planning, simulation and report writing:	Jean Morin [1] Olivier Champoux [1] Yves Secretan [2]
Input files of the temperature model:	Daniel Nadeau [2]
Revision:	André Bouchard [1]
SQL coding:	Sylvain Martin [1]
Linkage temperature/fish:	Marc Mingelbier [5] Philippe Brodeur [5]
Database queries for data on tributaries temperature:	Mario Bérubé [4]
Climatic data production:	Adrien Julien [3]

1: Environnement Canada, Service météorologique du Canada – Hydrologie (SMC Hydrologie).

2: Institut national de la recherche scientifique – Eau, Terre et Environnement (INRS-ETE)

3: Centre de Ressources en Impacts et Adaptation au Climat et à ses Changements. Service météorologique du Canada, Environnement Canada.

4: Direction du suivi de l'état de l'environnement, ministère de l'Environnement du Québec (MEQ).

5: Société Faune et Parc, Québec (FAPAQ).

TABLE OF CONTENTS

LIST OF FIGURES

LIST OF TABLES

1. Introduction

Water temperature is a crucial factor for aquatic life. For fish, water temperature directly influences their metabolism, physiology and behaviour (Wootton, 1998). Indirectly, it modifies the environmental characteristics of the habitat, such as gas dissolution (Wetzel, 2001). For fish, temperature is considered to be the main factor explaining the variability of year class strength (Koonce *et al*., 1977 ; Fortin *et al*., 1982).

Within the « Plan of study » of the International Joint Commission (IJC) on the Lake Ontario – St. Lawrence River (LOSLR), the Environment Group (ETWG) is responsible for quantifying the impacts on flora and fauna from regulation of discharge. One portion of these impacts is associated with water temperature. During spring time, Northern Pike use the warmest portions of the floodplain to spawn. The regulation of discharge has a direct influence on local water depth and the local water temperatures. As a consequence, the regulation of discharge will affect the reproduction of Northern Pike. In order to assess the impact of water temperatures on reproduction, we have to produce and include a temperature layer in 2D Suitable Habitat Index for fish spawning ground.

2D temperature modelling for the St. Lawrence River originated from two different projects completed in order to fulfill the IJC-ETWG modelling needs. The first project tested the possibility of using a 2D model to reproduce water temperatures observed in the Boucherville Island at Battures Tailhandier during the spring of 1999 (Morin *et al*., 2002). This project showed the possibility of reproducing the spatial and temporal pattern of temperature over the Tailhandier flats. The second project used a new set of water temperature data covering a larger portion of the flats representing spring conditions used by Northern pike for reproduction. In this second project, it was shown that the hourly temperature signal can be reproduced with a high-precision (fraction of a °C) both temporally and spatially. The high precision of the models allowed the utilization of simulated water temperature as an input into early spawners reproduction models (Morin *et al*., 2003).

Few studies have shown the spatio-temporal evolution of the temperature in the St. Lawrence River system. Recently, the H&H group (Hydrology&Hydraulics) of the IJC, was asked a series of question on water temperature, and Dr T. Shen's group have modelled the thermal budget of the river reach from Lake Ontario to the dam near Cornwall. They demonstrated that there is a very small to unsignificant effect of the discharge on the thermal regime in this portion of the river. For the simulation with the outflow increased by +200 m^3/s flow, the decrease in water temperature was approximately 0.04 ^0C (Dr T. Chen, N. Jayasundara and A. Thompson, Pers. Comm.). The conclusion of this study can only be applied for the main water mass of this fast flowing section that does not include an extensive floodplain. However, in the St. Lawrence River floodplain, mainly located downstream of Montréal, the discharge largely influences the extension of the flooded area. In these conditions, the thermal regime is strongly influenced by the local water depth and its temporal variations.

This report will focus on the modelling of the quarter-monthly mean water temperature over the area from Lake Saint-Louis to Trois-Rivières and its evolution during spring time. The objectives of the present study are 1) to produce a complete series of climatic data from 1953 to 2000, in quarter-month average, 2) to produce an "average climate" for the available climatic record, 3) to produce water temperature boundary conditions for the 2D modelling from the "average climate" and finally 4) to produce 16 quarter-month water temperature simulations during early spring for the mean climate and for 8 discharge scenarios covering the entire spectrum of possible hydrologic conditions. The report essentially describing the methodology used to produce the data set and water temperature simulations, while results are also briefly presented.

2. Methodology

2.1. Overview of the methodology

The objective of the study is to produce reliable 2D temperature simulations to be used for predicting spawning areas for Northern pike and Yellow perch. In this study, the focus is on the period of the year during which these fish species are spawning. The target period ranging from quarter-month (QM) 9 to 24 corresponding to the first QM of March to the last QM of June. The pre-determined QM temporal scale implies that we can consider the system in a permanent regime or steady state. In this system, neighbouring QM have no influence on each other because a QM is long enough to reach equilibrium with the climatic and boundary conditions. Also, in order to simplify the problem and to allow the interpolation of temperature results, the driving climatic conditions were considered spatially constant and based only on the Dorval station.

Climatic data needed to compute 2D temperature modelling are available only since 1953. Simulating all QM for all springs since this period represents a huge task that would produce a significant amount of data. In order to reduce and simplify the analysis, we have decided to work with a “normal” climate representing the interannual average of QM from QM 9 to 24 for all 8 discharge scenarios. The simplification produced a total of 16 QM simulated for 8 discharge scenarios, for a total of 128 temperature simulations covering the entire system from Lake Saint-Louis to Trois-Rivières. As shown further in this report, accumulated degree-days are strongly correlated with the water temperature of tributaries during spring time. Accumulated degree-days will be used as an interpolation tool to transfer simulated temperature QM-discharge scenarios to any QM needed for any year (in terms of discharge and accumulated degree-days).

The entire methodology can be divided into three main sections 1) the construction of the climatic series 2) the construction of the inflow temperature models and 3) the simulation of the 2D temperature model and each of these sections can be divided in the following tasks:

A: Construction of the climatic series:

1. Inventory of available data (daily mean);
2. Choice of a climatic station that is representative of the system, of data missing; identification and statistical analysis of correlations with nearby stations;
3. Completion of the daily series for all climatic parameters and averaging in QM;
4. Construction of the normal climate from averaging interannually QM data, including accumulated degree-days and construction of boundary conditions for QM 9 to QM 24.

B: Construction of the temperature models for tributaries and inflows and of boundary conditions construction:

1. Extraction of tributaries temperature data from the *Ministère de l'environnement du Québec* database;
2. Combination of the temperature database with discharge and accumulated degree-days databases;
3. Construction of 3 term relationships for all tributaries with a commercial statistical package (Statistica);
4. Production of boundary conditions for tributaries corresponding to discharge scenarios and accumulated degree-days for QM 9 to QM 24.

C: 2D temperature modelling:

1. Construction of the numerical field model and calculation grid (prior to this study);
2. Hydrology and elaboration of scenarios (prior to this study);
3. Hydrodynamic modelling (prior to this study);
4. Construction of climatic files driving the temperature model;
5. Construction of boundary conditions files for tributaries temperature;
6. Calibration and validation of diffusivity with satellite images;
7. Temperature modelling.

2.2. Historical reconstruction of meteorological data

For many years, several meteorological parameters have been measured at different stations. The longest time series for climatic data are generally located near major airports and are complete or are missing only short portions. After analysis of the temporal and spatial availability of all historical meteorological data for all the parameters and stations, Dorval station (station 7025250) was chosen as the primary station for driving the 2D water temperature model.

For complete series reconstruction, we have completed the series on a daily means basis and later reduced it for producing complete QM mean for each climatic parameter. The period used for the analysis is from January 1st 1953 to December 31st 2000. Several data were missing from Dorval station series and statistical correlations between stations were produced in order to complete the series. Also some parameters were not measured during a large portion of the series; we therefore built a model to reproduce these parameters with correlated data (cloud cover). More details on the completion methods are explained in the section describing results.

The following parameters were considered in the analysis:

1) Could cover;
2) Relative humidity;
3) Atmospheric pressure;
4) Air temperature;
5) Solar radiation;
6) Precipitation;
7) Wind velocity.

2.3. Temperature for tributaries and inflows

The St. Lawrence River water temperature is strongly influenced by the temperature of the inflowing tributaries. They have a major influence especially on riparian shallow

water areas. Water temperature data for several tributaries where collected by the *ministère de l'Environnement du Québec* and extracted from the *Banque de données sur la qualité du milieu aquatique.* The Figure 1 illustrates the tributary water temperature stations that were used. Water temperature measurements were used to produce simple predictive models linking discharge and accumulated degree-days. We used the available measure of temperature for the early portion of the year and only the data with a maximum of 600 degree-days.

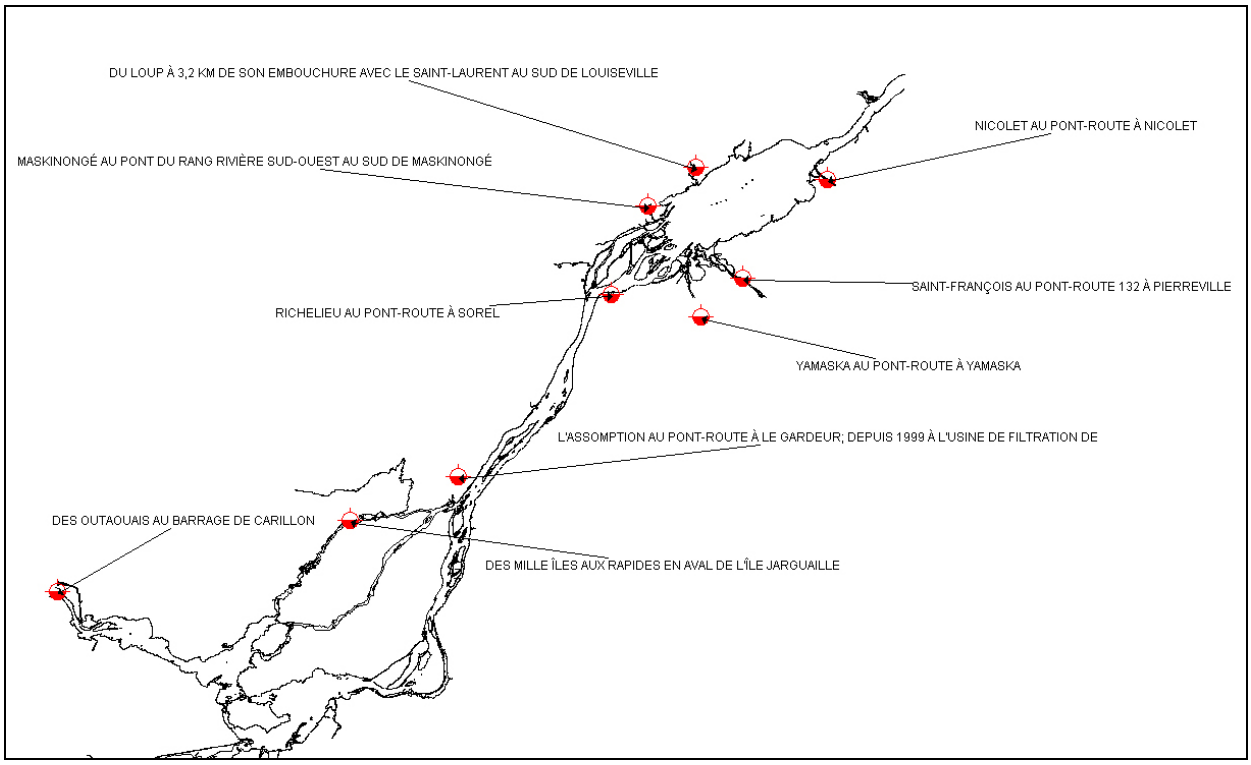

Figure 1: Location of temperature measurement stations associated with main tributaries.

2.4. 2D Temperature model: structure and use

2.4.1. Hydrology and numerical field model

Prior to this study, significant efforts have been invested into the simplification of the hydrologic characterization (Morin and Bouchard, 2001; Morin *et al.* 2003) by the use of discharge scenarios. These scenarios where used for bidimensional simulations of the

most important physical drive of the system, such as hydrodynamics, wind waves, light penetration and other physical variables of the St. Lawrence River ecosystem. The uses of the hydrological scenarios allow the production of water temperature simulations that covers the entire spectrum of St. Lawrence River spring hydraulicity with a relatively small number of simulations. Detailed methodologies on digital terrain model preparation, hydrodynamic modelling and calibration and validation of hydrodynamic models can be found in Morin *et al.* (2001; 2002; 2003).

2.4.2. Hydrodynamic model

The hydrodynamic results are fundamental information that is used by the water temperature model. Hydrodynamic modelling was performed using the HYDROSIM model developed at INRS-Eau (Leclerc *et al.* 1995). The approach used is based on the two-dimensional finite element discretisation of the St. Venant equations (flux formulation), which are solved using an iterative transient solution method named Euler-GMRES (Heniche *et al.* 1999). It solves simultaneously the mass and momentum conservation principles, and takes into account the local friction coefficient for parameterization. The turbulence closure scheme uses the mixing length theory (0-equation model) which involves the horizontal velocity gradients. Vertically integrated, the model produces reliable predictions of mean velocity of the water column, water level, and specific discharge for a wide range of hydrological conditions. The model solves the wetted surface since it incorporates a drying-wetting functionality that allows dynamical estimates of the flow boundary.

As one seeks the steady-state conditions, the solution is considered independent of the initial conditions. As for the boundary conditions scheme, one usually solves the problem using a specified discharge at the upstream boundary, water level at the main outlet and specified discharges at the tributary and secondary outlets. Moreover, tangent velocities are imposed as null. For a closed lateral boundary, the drying-wetting functionality is equivalent to imposing a zero normal flux and a slip flow condition.

2.4.3. Water temperature model

In natural, rivers water temperature is mainly controlled by climatologic parameters like: solar radiation, air temperature, atmospheric pressure, relative humidity, precipitation and wind velocity (Heniche *et al.* 2002). Transport-diffusion partial derived equations (Secretan *et al.* 2000) are the basic equations of a water temperature model. Water temperature simulation capabilities are added to the equations by implementing the water column heat balance. This addition helps in the identification within the model of all heat sources and sinks. Thus, the total heat flow rate *S* contributing in the heat balance of the water column can be expressed as:

$$S = S_a + S_b + S_i$$

where S_a, S_b and S_i are respectively heat flow rates between the atmosphere, between the river bed and between the ice cover.

Atmospheric heat flow rate S_a is normally the most important in the total heat flow rate *S*. The atmospheric heat flow is calculated by solar radiation, infrared radiation evaporation, convection and precipitation:

$$S_a = (H_s - H_l - H_e - H_c - H_p) f_{extinc}$$

weighted by an extinction f_{extinc} function.

The river bed heat flow rate can be an important factor, especially into shallow water areas. Determination of S_b can be very challenging. To help with the determination of S_b underground temperature was considered as constant and the thermal convection law was used to represent the heat flux rate with the river bed:

$$S_b = -K_b(T - T_b)$$

where K_b and T_b are respectively the heat flux coefficient and underground temperature.

In northern cold areas, the estimation of the ice cover's heat flux rate is mandatory. The estimation of the heat flux is done with the following relationship, with negligible frazil ice concentration hypothesis:

$$S_i = -K_i(T - T_m)$$

where K_i is the heat flux coefficient.

2.4.4. Mathematical model

A depth-averaged bidimensional transport-diffusion equation forms the basis of the water temperature model. With the hypothesis of steady state hydrodynamic conditions, the partial differential equation in non-conservative format is:

$$H\frac{\partial T}{\partial t} + H\left(u\frac{\partial T}{\partial x} + v\frac{\partial T}{\partial y}\right) - \frac{\partial}{\partial x}H\left(D_{xx}\frac{\partial T}{\partial x} + D_{xy}\frac{\partial T}{\partial y}\right) - \frac{\partial}{\partial y}H\left(D_{yx}\frac{\partial T}{\partial x} + D_{yy}\frac{\partial T}{\partial y}\right) + QH(T - T^0) - \frac{S}{\rho c_p} = 0$$

where t and (x, y) are time and cartesian coordinates ; T, is the depth averaged temperature (unknown); H water depth ; u and v are the velocity components ; Q heat discharge by volume unit coming from tributaries or underground sources, and T_0 its temperature. In the last term, S, ρ and c_p are heat flux rates presented earlier, the density and the water specific heat. Dispersion coefficients D_{xx}, D_{yy}, $D_{xy}=D_{yx}$ are derived form the hydrodynamic results and are adjusted during the calibration process to represent observed data.

This complex equation system is temporally resolved after imposing boundary conditions and providing an initial solution to the system. Water temperature at the inflow boundary is considered as a function of time while at the outflow, it is considered free condition to be a ($\partial T/\partial \boldsymbol{n} = 0$). Moreover, in dried zones, water temperature and water depth are imposed at zero.

Numerical implementation

The water temperature model uses two types of properties, the global properties and the nodal properties. The global properties are time and space constants (Table 1) while the nodal properties (Table 2) can have different values for each calculated node in the

domain. For calculation and optimisation purposes, it was decided to use a maximum of global properties (physical data) whenever possible.

Table 1: Global properties of the temperature model

Diffusivity	Water Properties	Ice Properties	Meteorological data	Field data	Regression coefficients
D_M, β_V, β_H, β_L	ρ, c_p	ρ_i, c_{pi}, L_i	P_{atm}	T_b	A_l, B_l

The

Table 1 lists the 13 global properties:

- Molecular dispersion D_M;
- Dispersion weighting coefficient β_V, β_H and β_L;
- Water properties ρ and c_p;
- Ice properties ρ_i, c_{pi} and L_i;
- Atmospheric pressure P_{atm};
- Underground temperature T_b ;
- Regression coefficient A_l and B_l.

Table 2: Nodal properties of the temperature model

Field data	Hydrodynamic data	Meteorological data
K_b, SF, r	u, v, H, D_H, D_V	H_{si}, T_a, ε_a, RH, f(W_z), p_r or p_s, K_i, f_{extinc}

Table 2 shows the 16 selected nodal properties for field (3), hydrodynamic (5) and meteorological (11). Field data include:

- River bed heat flux rate coefficient K_b;
- Vegetation cover (in %) *SF* ;
- Water turbidity *r*.

Hydrodynamic data include:

- Water velocity component u and v;
- Water depth H;
- Dispersion coefficient D_H and D_v.

Meteorological data and derived variables include:

- Solar radiation H_{si} ;
- Air temperature T_a ;
- Air emissivity ε_a;
- Relative humidity RH ;
- Wind function $f(W_z)$;
- Precipitation : rain p_r if $T_a \geq 0$ ℃ or snow p_s if $T_a < 0$ ℃ ;
- Ice cover heat flux rate coefficient K_i;
- Extinction function f_{extinc}.

3. Results

3.1. Synthetic climatic series for the St. Lawrence River; completion of climatic data at Dorval station

3.1.1 Cloud cover

The time-series of cloud cover was recorded at Dorval station for the entire period (1953-2000). No missing data were observed for the daily values. No other post-processing was performed on cloud cover data. Figure 2 presents the daily cloud cover for the entire period (1953-01-01 to 2000-12-31).

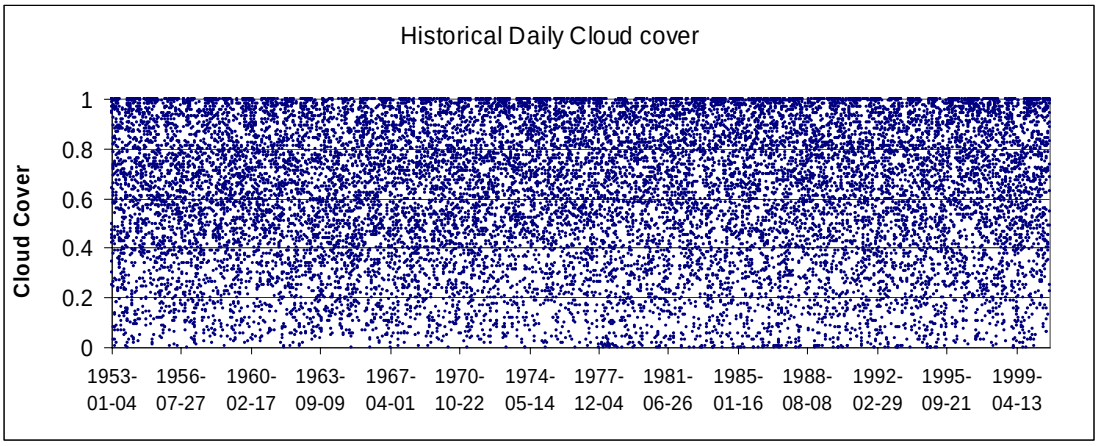

Figure 2: Complete series of the daily cloud cover for Dorval station.

3.1.2. Relative humidity

The time-series of relative humidity was recorded at Dorval station for the entire period (1953-2000). No missing data were observed for the daily value. No other post-processing was performed on Relative humidity data. Figure 3 presents the relative humidity for the entire period (1953-01-01 to 2000-12-31).

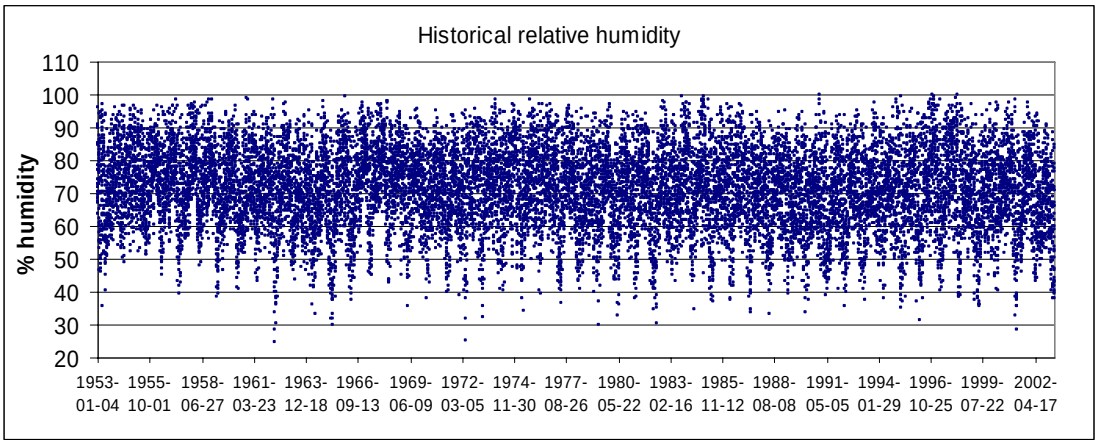

Figure 3: Complete series of the relative humidity for Dorval station.

3.1.3. Atmospheric pressure

The time-series of atmospheric pressure was recorded at Dorval station for the entire period of interest. Missing data were observed in the daily values. Missing data replacement was performed using atmospheric pressure data measured at the Saint-Hubert station which is the closest station with long time series. The correspondence of atmospheric pressure between the two stations was calculated with observed daily data. Figure 4 illustrates the results of the correspondence analysis.

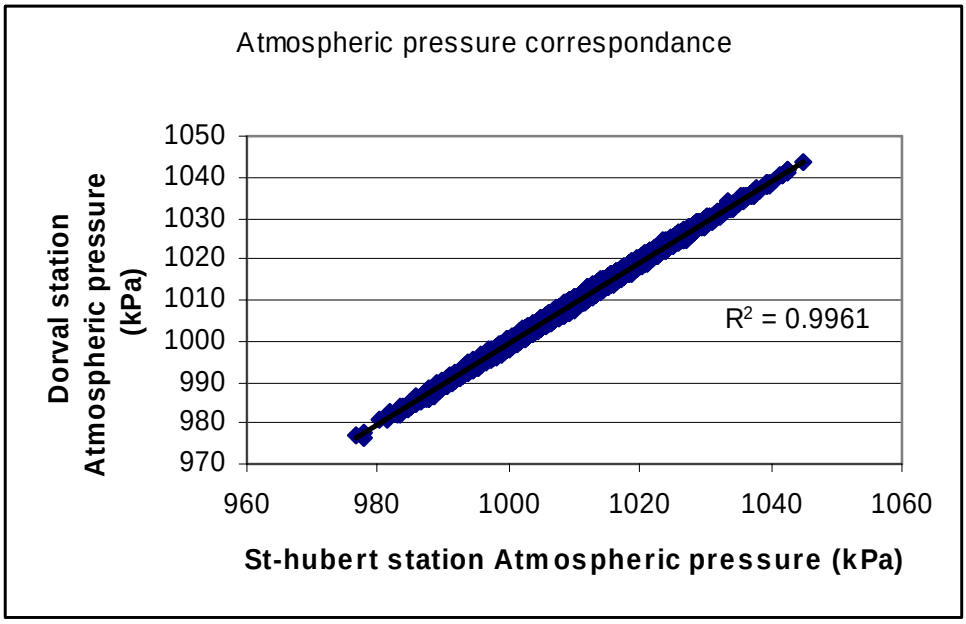

Figure 4: Relation between daily atmospheric pressure at Dorval and Saint-Hubert stations.

Figure 5 shows the results of the missing data replacement exercise for the atmospheric pressure at Dorval station with Saint-Hubert station data. The missing data replacement procedure produced a complete series of daily values for the entire period (1953-01-01 to 2000-12-31).

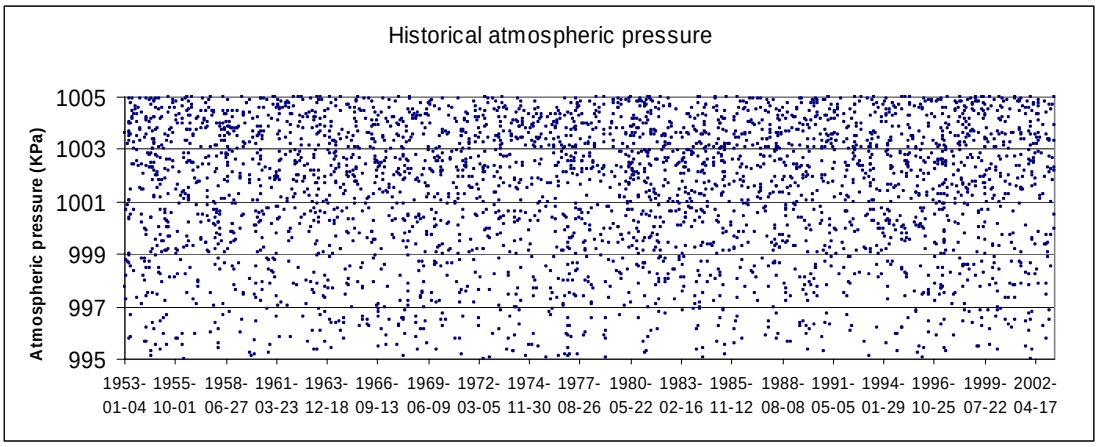

Figure 5: Complete series of the daily atmospheric pressure for Dorval station.

3.1.4. Air temperature

The time-series of air temperature was recorded at Dorval station for the entire period (1953-2000). No missing data were observed for the daily values. No other post-processing was performed on this series. Figure 6 presents the air temperature for the entire period (1953-01-01 to 2000-12-31).

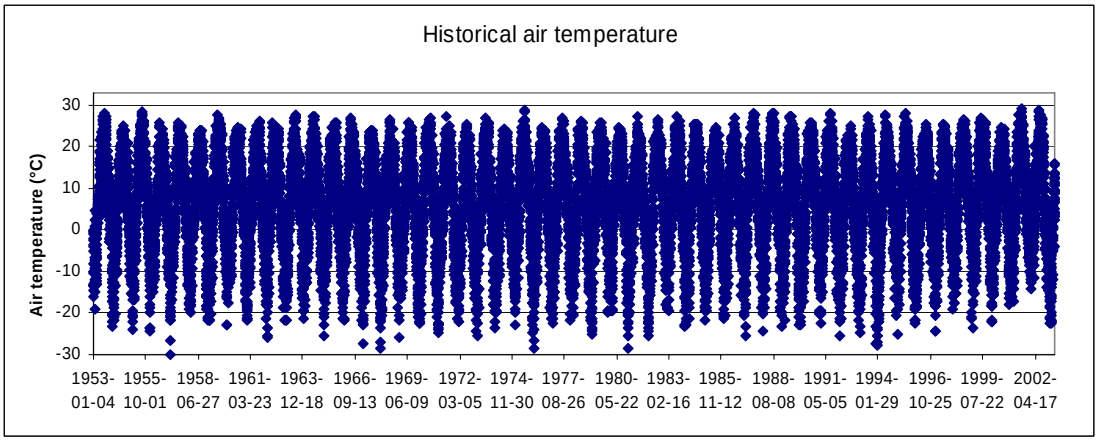

Figure 6: Complete series of the daily air temperature for Dorval station.

3.1.5. Solar radiation

Solar radiation data measured at Dorval station is the series with the most important number of missing data points. The only available data that could be used to fill in cover the period between 1988 and 2003 and no other station can provide data for the missing period. Reconstruction of solar radiation was produced by using relationships between theoretical daily solar radiations during the year and observed cloud opacity. Cloud opacity is qualitative data, estimated on a 0 to 10 scale. Both solar radiation and cloud cover are available for the portion 1988 to 2000 of the series. The theoretical function for the maximum solar radiation during the year was built using the interannual maximum measurements of the solar radiation from the available data. A polynomial equation properly reproduces the annual cycle (Figure 7) observed in the solar radiation data.

The relation between cloud opacity and solar radiation was built using the ratio of theoretical radiation and measured radiation on measured opacity (Figure 8). The resulting relationship is used to modulate the theoretical solar radiation with the cloud opacity for all the time-steps within the considered period. The validation with measured solar radiation gives a satisfactory result. Figure 9 illustrates the high degree of correspondence (r^2=0.85) between simulated and measured solar radiation. The completed solar radiation series is shown in Figure 10.

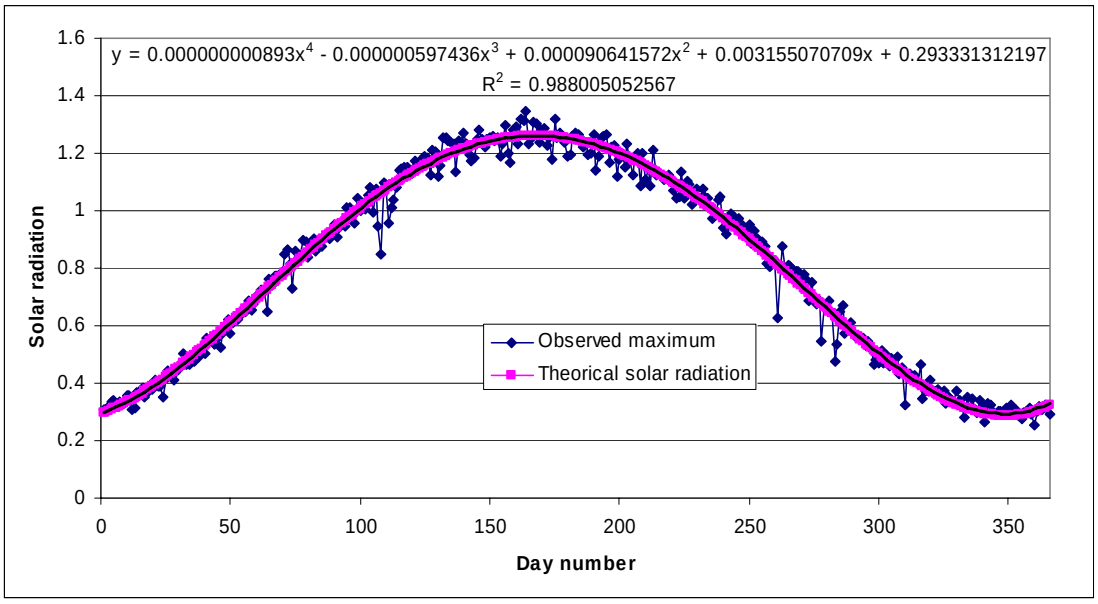

Figure 7: Historical maximum value for measured solar radiations and theoretical model for Dorval station.

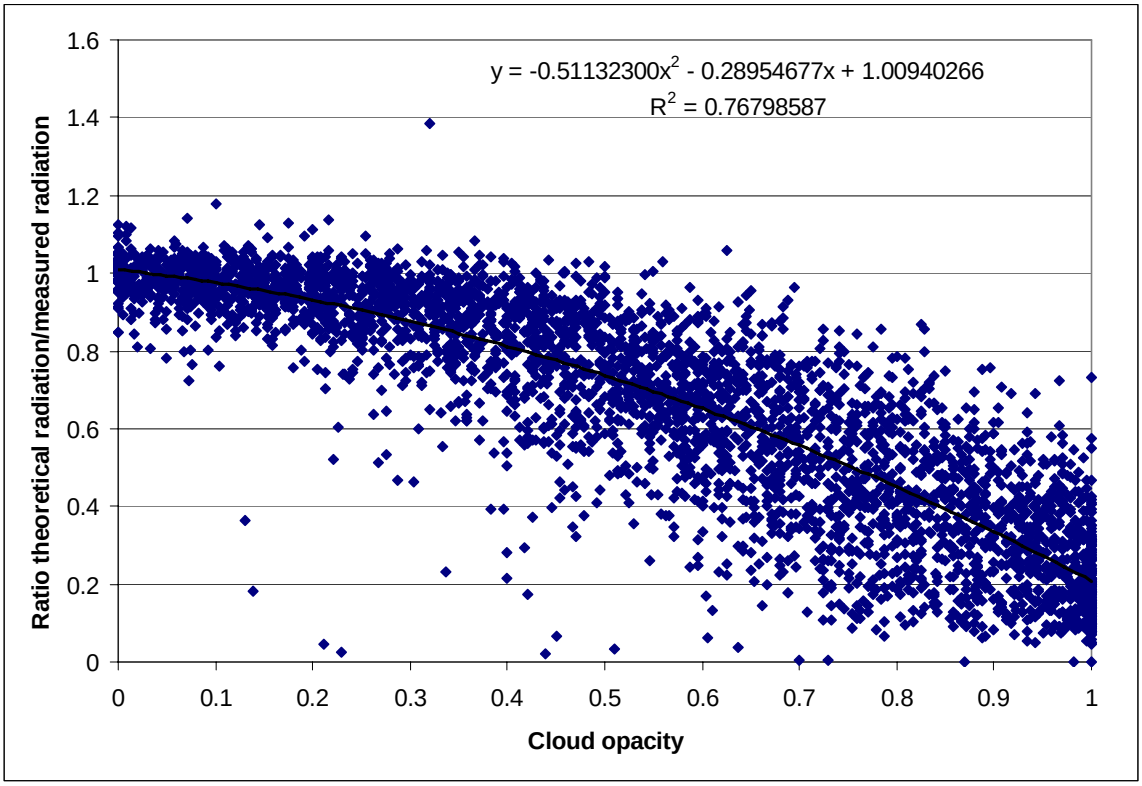

Figure 8: Relation between observed cloud opacity and the ratio between “theoretical/measured radiations”.

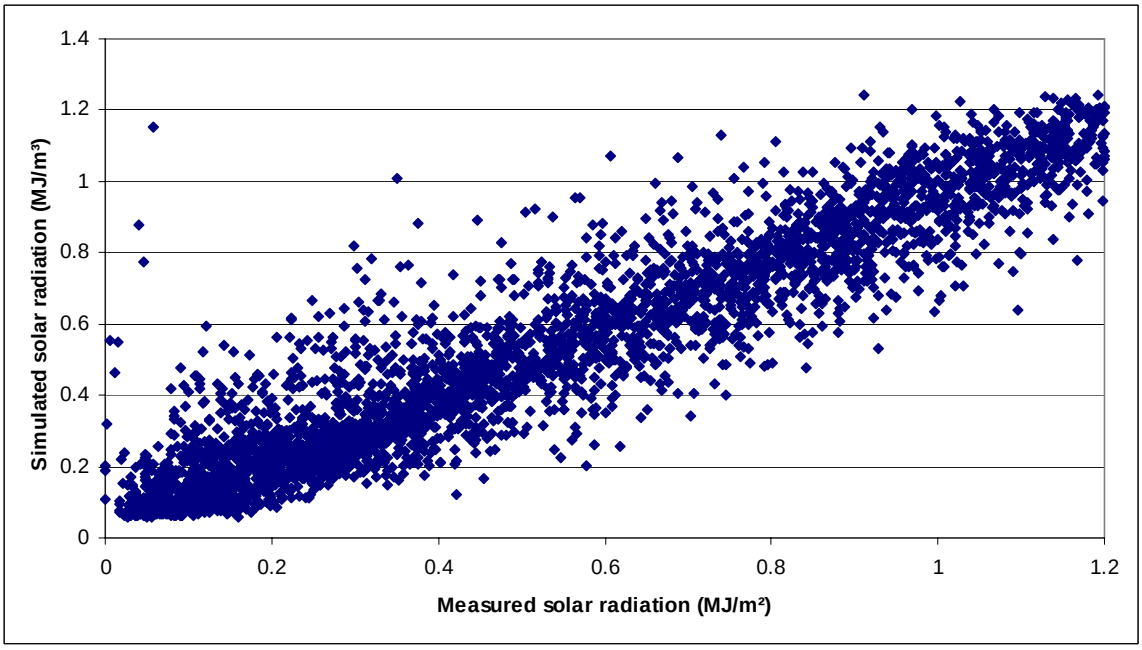

Figure 9: Relation between simulated and measured solar radiation for the validation period for Dorval station.

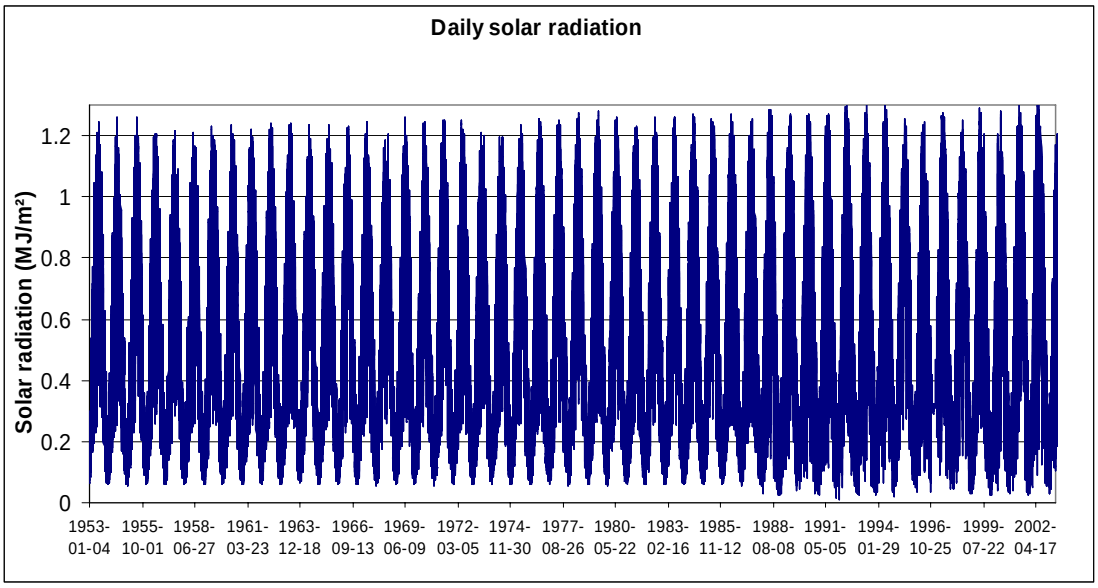

Figure 10: Complete series of the daily solar radiation for Dorval station.

3.1.6. Precipitation

The time-series of precipitation was recorded at Dorval station for the entire period of interest. No missing data were observed for the daily values. No other post-processing was performed on these data. Figure 11 presents the precipitation for the entire period (1953-01-01 to 2000-12-31).

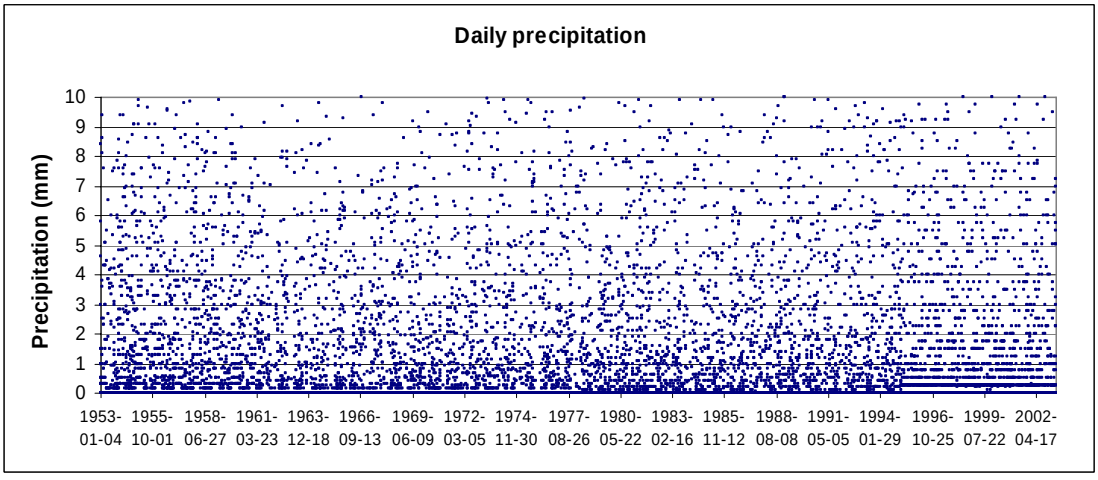

Figure 11: Complete series of the daily precipitation for Dorval station.

3.1.7. Wind velocity

The time-series of wind velocity was recorded at Dorval station for the entire period of interest. No missing data were observed for daily values. No other post-processing was performed on wind velocity data. Figure 12 presents the precipitation data for the entire period (1953-01-01 to 2000-12-31).

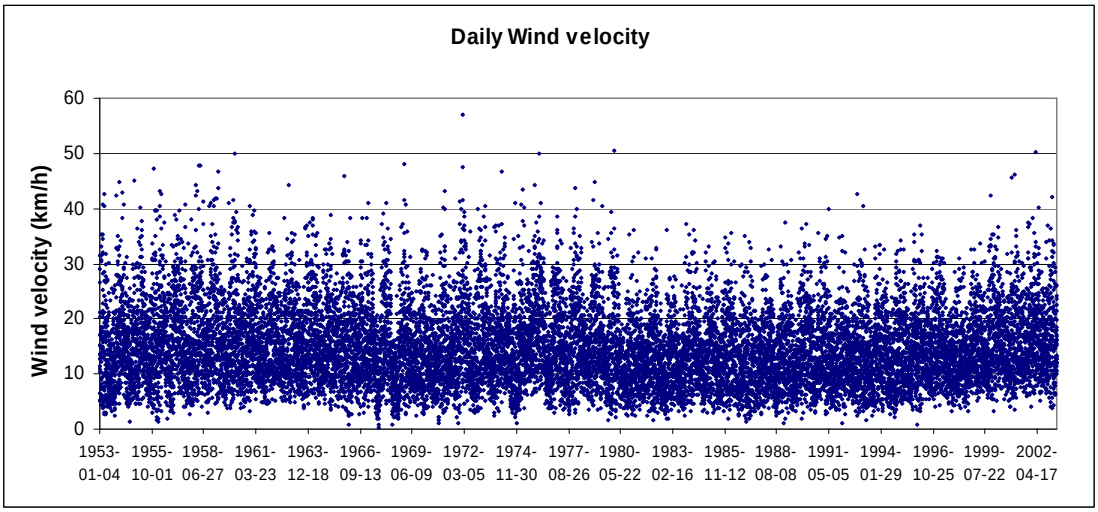

Figure 12: Complete series of the daily wind intensity for Dorval station.

3.2. Temperature boundary conditions for the tributaries and main inflow

3.2.1. Ottawa River (Carillon Dam)

Figure 13 presents the relationship produced for the Ottawa River at Carillon. The relationship between accumulated degree-days (ADD), discharge and water temperature is highly significant (r^2=0.9655). Validation of the relationship was performed with measured water temperature. Figure 13 presents the results of the validation.

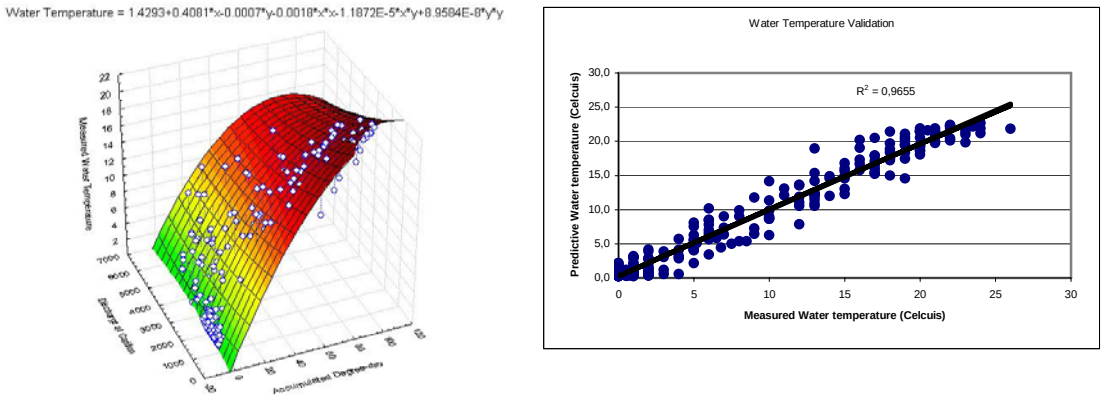

Figure 13: Relation between degree-days, discharge and water temperature for the Ottawa River and the validation of the resulting model.

3.2.2. Des Milles-Îles and des Prairies Rivers

Because of the hydrological link between the Ottawa River at Carillon and the des Milles-Iles and des Prairies Rivers, the water temperature of des Milles-Iles and des Prairies Rivers was directly compared to measured water temperature at Carillon to produce a relationship based on water temperature at Carillon. Figure 14 presents the relationship between Carillon and des Milles-Îles River.

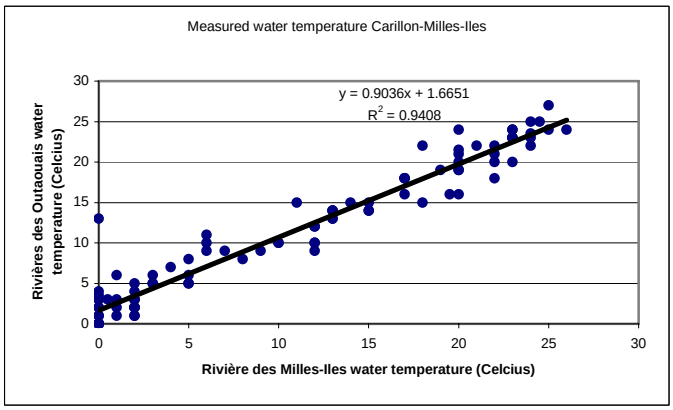

Figure 14: Relation between Ottawa River and the des Milles-Îles River temperature.

3.2.3. L'Assomption River

Figure 15 presents the relationship produced for L'Assomption River. The relationship between ADD, discharge and water temperature is highly significant (r^2=0.88).

Validation of the relationship was performed with measured water temperatures. Figure 15 presents the results of the validation.

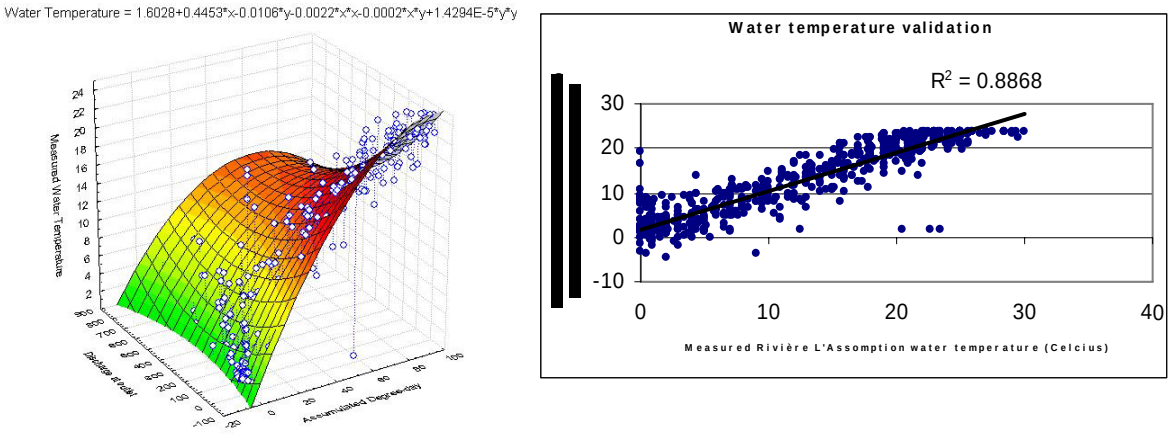

Figure 15: Relation between degree-days, discharge and water temperature for L'Assomption River and the validation of the resulting model.

3.2.4. Richelieu River

Figure 16 presents the relationship produced for the Richelieu River. The relationship between ADD, discharge and water temperature is highly significant (r^2=0.87). Validation of the relationship was performed with measured water temperature. Figure 16b presents the results of the validation.

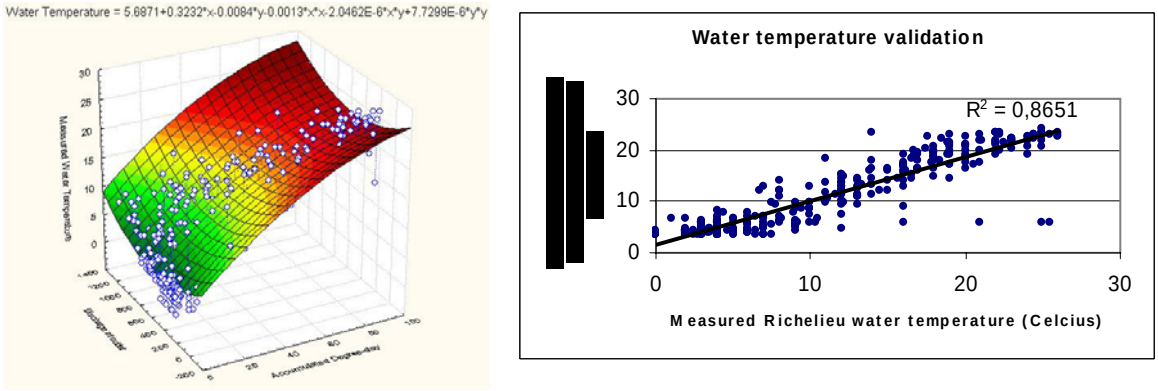

Figure 16: Relation between degree-days, discharge and water temperature for the Richelieu River and the validation of the resulting model.

3.2.5. Yamaska River

Figure 17 presents the relationship produced for the Yamaska River. The relationship between ADD, discharge and water temperature is highly significant (r^2=0.85). Validation of the relationship was performed with measured water temperature. Figure 17b presents the results of the validation.

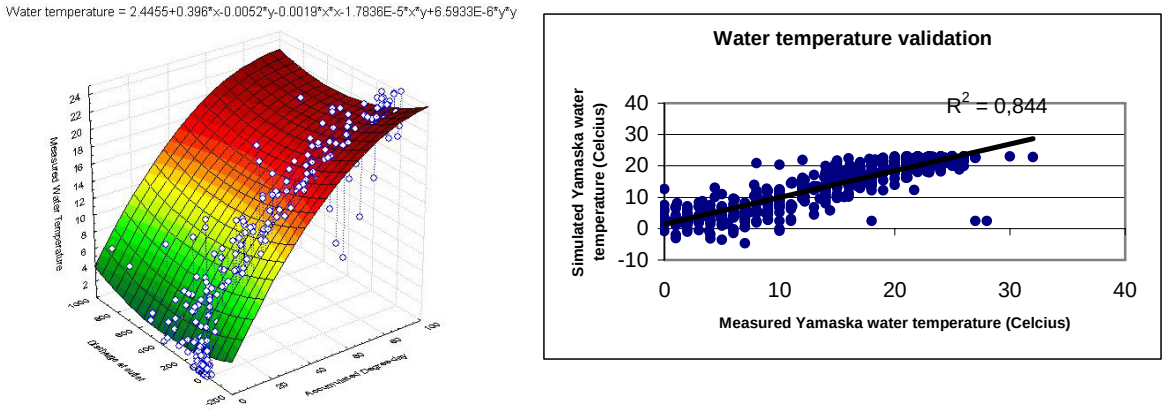

Figure 17: Relation between degree-days, discharge and water temperature for the Yamaska River and the validation of the resulting model.

3.2.6. Saint-François River

Figure 18 presents the relationship produced for the Saint-François River. The relationship between ADD, discharge and water temperature is highly significant (r^2=0.87). Validation of the relationship was performed with measured water temperature. Figure 18 presents the results of the validation.

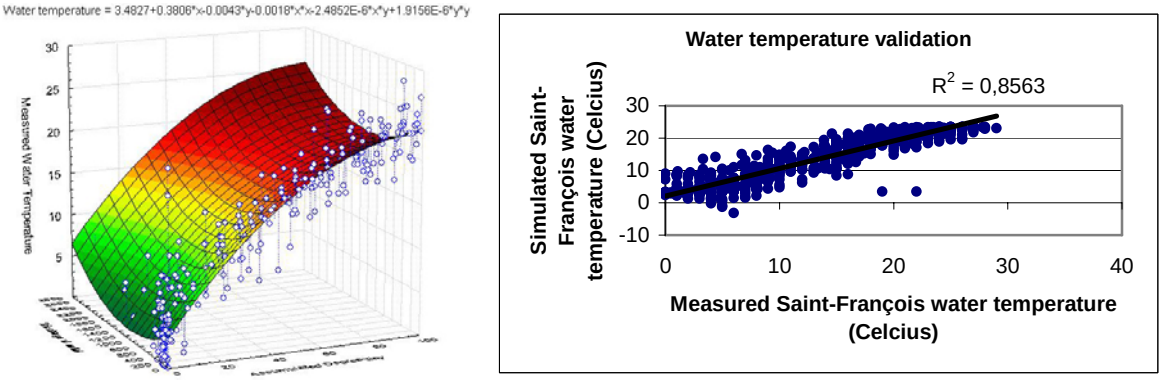

Figure 18: Relation between degree-days, discharge and water temperature for the Saint-François River and the validation of the resulting model.

3.2.7. Nicolet River

Figure 19 presents the relationship produced for the Nicolet River. The relationship between ADD, discharge and water temperature is highly significant (r^2=0.88). Validation of the relationship was performed with measured water temperature. Figure 19 presents the results of the validation.

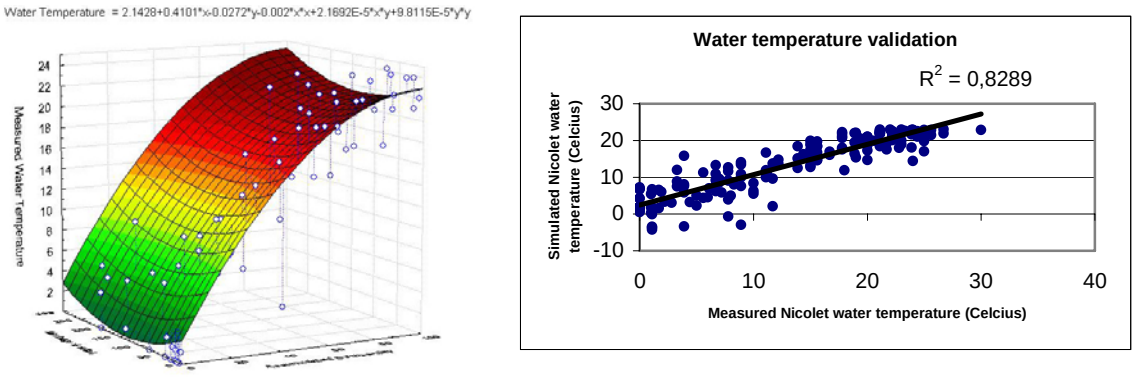

Figure 19: Relation between degree-days, discharge and water temperature for the Nicolet River and the validation of the resulting model.

3.2.8. Du Loup River

Figure 20 presents the relationship produced for the DuLoup River. The relationship between ADD, discharge and water temperature is highly significant (r^2=0.94). Validation of the relationship was performed with measured water temperature. Figure 20 presents the results of the validation.

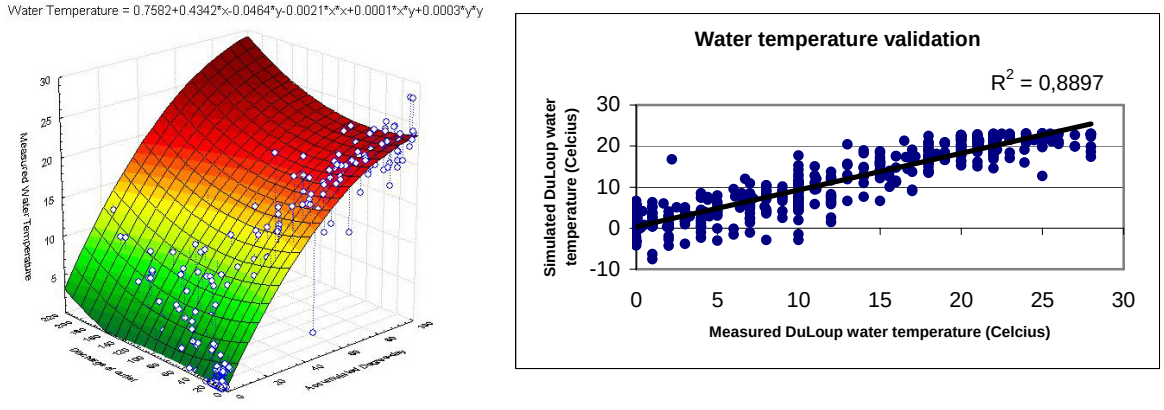

Figure 20: Relation between degree-days, discharge and water temperature for the Du Loup River and the validation of the resulting model.

3.2.9. Maskinongé River

Figure 21 presents the relationship produced for the Maskinongé River. The relationship between ADD, discharge and water temperature is highly significant (r^2=0.94). Validation of the relationship was performed with measured water temperature. Figure 21 presents the results of the validation

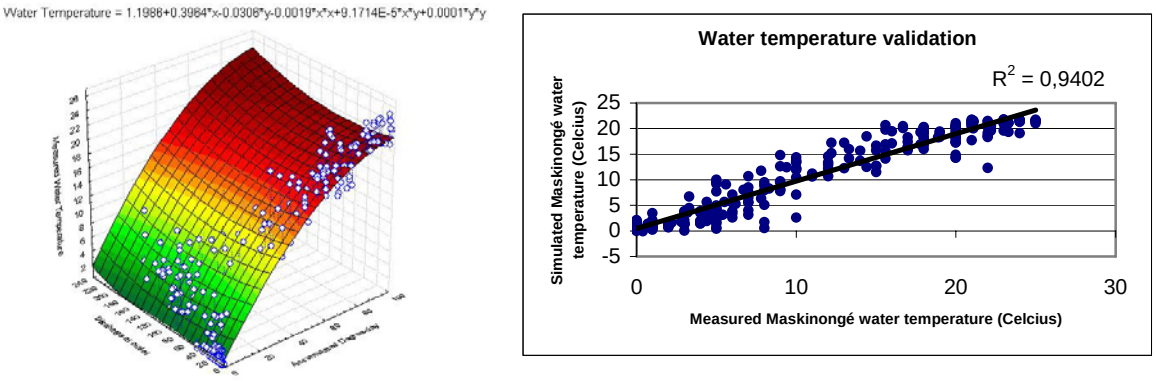

Figure 21: Relation between degree-days, discharge and water temperature for the Maskinongé River and the validation of the resulting model.

3.2.10. St. Lawrence River at Beauharnois Dam

Figure 22 presents the relationship produced for the St. Lawrence River at the Beauharnois Dam. The relationship between ADD, discharge and water temperature is highly significant (r^2=0.92). Validation of the relationship was performed with measured water temperature.

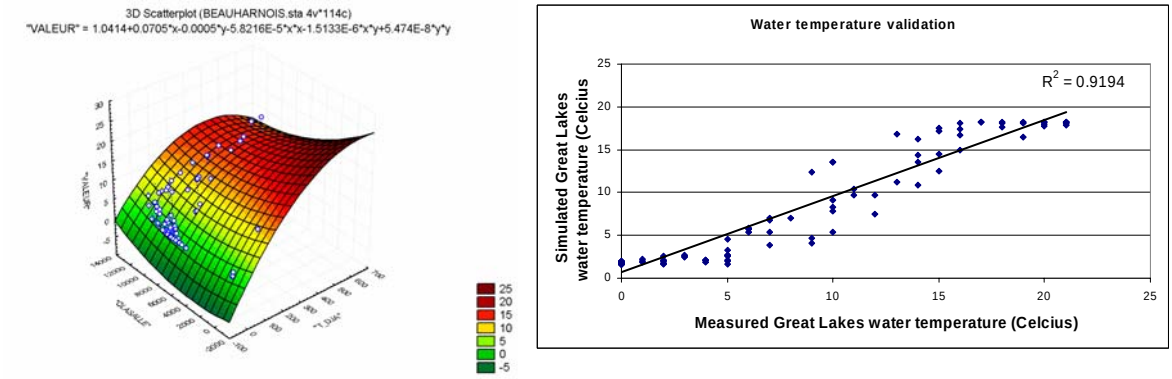

Figure 22: Relation between degree-days, discharge and water temperature for the St. Lawrence River at Beauharnois Canal and the validation of the resulting model.

3.3. Boundary conditions for each quarter-month for 2D temperature simulations

3.3.1. Global meteorological modeling conditions (QM aggregation)

In order to feed the water temperature model in global and nodal properties, and to meet the Plan of study temporal step, daily meteorological parameters where reduced to QM mean (from the reconstructed daily series) for each QM (1 to 48) of each year. For the 2D simulations we used the "normal" climate, which is the average interannual QM from the available climatic series. Table 3 presents these QM means (normal climate) for the spring time period used in the water temperature model. The QM is used to cover the entire fish spawning spring period.

Table 3: Climatic conditions used for driving the 2D temperature model in these conditions were used as spatially constant over the entire system.

Quarter month	Cloud Cover %	Relative Humidity %	Atmospheric pressure kPa)	Air temperature (oC)	Solar Radiation (MJ)	Precipitation (mm/day)	Wind Velocity (km/h)
9	0.64	71.26	1010.97	-4.68	0.45	0.06	17.40
10	0.65	70.05	1011.39	-3.56	0.50	0.05	16.26
11	0.60	69.36	1010.71	-1.35	0.58	0.05	16.26
12	0.60	67.97	1011.03	1.30	0.61	0.05	16.51
13	0.67	69.10	1008.37	2.66	0.59	0.07	16.85
14	0.59	63.96	1010.82	4.59	0.68	0.05	16.53
15	0.65	65.64	1009.62	7.52	0.67	0.06	16.15
16	0.63	62.90	1010.26	9.03	0.73	0.05	15.30
17	0.61	61.03	1010.25	10.91	0.78	0.07	15.21
18	0.64	64.05	1009.47	12.83	0.77	0.05	15.15
19	0.61	64.78	1009.78	14.52	0.82	0.05	14.25
20	0.61	65.15	1009.51	15.55	0.84	0.05	13.80
21	0.62	67.52	1008.74	16.63	0.84	0.06	13.60
22	0.60	67.71	1008.48	18.06	0.87	0.05	14.11
23	0.59	68.66	1008.98	19.43	0.89	0.06	13.32
24	0.60	69.40	1008.60	19.97	0.86	0.07	13.77

3.3.2. Tributaries water temperature boundary conditions (QM aggregation)

Water temperatures for the tributaries were calculated with the developed relationships presented earlier. The water temperature is a function of accumulated degree-days (ADD) and tributary discharge. In order to feed the relationships, the ADD was previously calculated with daily air temperature data for the entire reconstructed series. ADD was defined as the number of ^{o}C over 5^{o}C. Each daily QM value of each year was aggregated using the QM number. To determine the typical ADD of each quarter-month, the mean value of the ADD was used. The predetermined discharge within the hydrological scenarios (Morin and Bouchard 2001; Morin *et al.* 2003) were used in the tributaries water temperature relationships.

Quarter-monthly water temperature simulations

To produce reliable water temperature simulations usable for fish spring spawning, all determined QM (9 to 24) were combined to the hydrological spring scenarios (8 scenarios) that cover the entire spectrum of spring hydraulicity. Thus, the total number of simulations (128) can be used for any meteorological or hydrological conditions by using linear interpolation between simulations representing specific conditions. is presents all the water temperature simulation (tributaries water temperature) by hydrological scenarios (1P to 8P) and by QM during spring time (9 to 24). is presents the accumulated degree days of the normal climate corresponding to the simulated conditions of the QM 9 to QM 24.

Table 4: Water temperature boundary conditions used for all 128 temperature simulations (2D).

1P											
QM	Outaouais	Chateaugu	Beauharnois	MIP	Assomption	Richelieu	Yamaska	St-Francois	Nicolet	DuLoup	Maskinongé
9	1.16	1.56	0.00	2.98	1.56	4.99	2.43	3.11	1.84	0.46	1.11
10	1.22	1.63	0.02	3.03	1.63	5.04	2.49	3.17	1.90	0.53	1.18
11	1.33	1.74	0.12	3.11	1.74	5.14	2.59	3.27	2.01	0.64	1.28
12	1.65	2.07	0.42	3.36	2.07	5.42	2.90	3.57	2.33	0.99	1.59
13	2.16	2.61	0.90	3.75	2.61	5.87	3.41	4.06	2.86	1.54	2.10
14	2.87	3.36	1.57	4.31	3.36	6.50	4.11	4.73	3.59	2.31	2.81
15	4.12	4.66	2.74	5.27	4.66	7.60	5.33	5.91	4.85	3.66	4.03
16	5.63	6.25	4.17	6.44	6.25	8.94	6.81	7.34	6.39	5.29	5.52
17	7.34	8.04	5.78	7.77	8.04	10.44	8.49	8.95	8.12	7.13	7.20
18	9.12	9.88	7.45	9.14	9.88	12.00	10.21	10.62	9.91	9.03	8.94
19	10.84	11.67	9.07	10.48	11.67	13.50	11.88	12.23	11.63	10.86	10.61
20	12.36	13.23	10.50	11.66	13.23	14.81	13.34	13.64	13.14	12.46	12.08
21	13.79	14.70	11.84	12.77	14.70	16.04	14.70	14.96	14.54	13.96	13.45
22	15.12	16.05	13.09	13.79	16.05	17.18	15.96	16.18	15.83	15.34	14.71
23	16.35	17.29	14.24	14.75	17.29	18.21	17.11	17.30	17.01	16.60	15.87
24	17.48	18.42	15.30	15.62	18.42	19.16	18.16	18.32	18.08	17.75	16.93

2P											
QM	Outaouais	Chateaugu	Beauharnois	MIP	Assomption	Richelieu	Yamaska	St-Francois	Nicolet	DuLoup	Maskinongé
9	0.78	1.53	0.55	2.68	1.53	4.90	2.42	3.08	1.79	0.42	1.09
10	0.84	1.60	0.60	2.73	1.60	4.96	2.48	3.14	1.85	0.49	1.15
11	0.94	1.71	0.70	2.81	1.71	5.05	2.58	3.24	1.96	0.60	1.25
12	1.25	2.04	1.00	3.05	2.04	5.33	2.90	3.54	2.29	0.95	1.57
13	1.75	2.58	1.48	3.44	2.58	5.78	3.40	4.03	2.81	1.50	2.07
14	2.45	3.33	2.14	3.98	3.33	6.42	4.10	4.70	3.54	2.28	2.78
15	3.66	4.64	3.30	4.92	4.64	7.52	5.33	5.88	4.81	3.62	4.01
16	5.14	6.22	4.71	6.06	6.22	8.85	6.81	7.31	6.34	5.25	5.49
17	6.81	8.01	6.31	7.36	8.01	10.36	8.48	8.92	8.07	7.09	7.17
18	8.54	9.85	7.96	8.70	9.85	11.91	10.21	10.58	9.86	8.99	8.91
19	10.22	11.64	9.56	10.00	11.64	13.42	11.87	12.19	11.58	10.82	10.58
20	11.69	13.21	10.98	11.14	13.21	14.73	13.34	13.61	13.09	12.43	12.06
21	13.08	14.67	12.30	12.21	14.67	15.96	14.70	14.93	14.49	13.92	13.42
22	14.36	16.02	13.53	13.20	16.02	17.10	15.95	16.15	15.78	15.30	14.69
23	15.54	17.26	14.67	14.12	17.26	18.14	17.10	17.27	16.97	16.56	15.85
24	16.63	18.40	15.71	14.96	18.40	19.08	18.15	18.29	18.04	17.71	16.91

3P											
QM	Outaouais	Chateaugu	Beauharnois	MIP	Assomption	Richelieu	Yamaska	St-Francois	Nicolet	DuLoup	Maskinongé
9	0.47	1.38	0.79	2.44	1.38	4.25	2.37	3.04	1.68	0.30	0.92
10	0.53	1.44	0.85	2.49	1.44	4.30	2.43	3.10	1.74	0.37	0.98
11	0.63	1.56	0.95	2.56	1.56	4.40	2.54	3.20	1.85	0.49	1.08
12	0.93	1.89	1.24	2.80	1.89	4.68	2.85	3.50	2.17	0.83	1.40
13	1.42	2.43	1.71	3.18	2.43	5.13	3.35	3.99	2.69	1.38	1.90
14	2.10	3.18	2.38	3.71	3.18	5.77	4.06	4.66	3.42	2.16	2.61
15	3.28	4.49	3.53	4.62	4.49	6.88	5.28	5.84	4.69	3.51	3.84
16	4.72	6.07	4.93	5.74	6.07	8.22	6.76	7.26	6.23	5.14	5.33
17	6.35	7.86	6.51	7.00	7.86	9.73	8.43	8.88	7.96	6.98	7.01
18	8.02	9.71	8.15	8.30	9.71	11.30	10.16	10.54	9.75	8.88	8.75
19	9.65	11.50	9.74	9.56	11.50	12.81	11.82	12.15	11.47	10.71	10.43
20	11.08	13.07	11.14	10.66	13.07	14.14	13.28	13.57	12.98	12.32	11.90
21	12.41	14.53	12.45	11.69	14.53	15.38	14.64	14.89	14.38	13.82	13.28
22	13.64	15.89	13.67	12.65	15.89	16.52	15.90	16.10	15.67	15.20	14.54
23	14.78	17.13	14.79	13.53	17.13	17.57	17.05	17.23	16.86	16.46	15.71
24	15.81	18.27	15.82	14.33	18.27	18.53	18.10	18.25	17.93	17.61	16.77

4P											
QM	Outaouais	Chateaugu	Beauharnois	MIP	Assomption	Richelieu	Yamaska	St-Francois	Nicolet	DuLoup	Maskinongé
9	0.29	1.23	0.80	2.31	1.23	3.76	2.30	2.98	1.54	0.30	0.86
10	0.35	1.30	0.86	2.35	1.30	3.82	2.36	3.04	1.61	0.37	0.92
11	0.45	1.41	0.95	2.43	1.41	3.91	2.46	3.14	1.72	0.49	1.03
12	0.75	1.74	1.24	2.66	1.74	4.20	2.78	3.44	2.04	0.83	1.34
13	1.22	2.28	1.71	3.03	2.28	4.65	3.28	3.93	2.56	1.38	1.85
14	1.89	3.03	2.37	3.54	3.03	5.29	3.98	4.60	3.29	2.16	2.55
15	3.05	4.34	3.51	4.44	4.34	6.41	5.20	5.78	4.56	3.51	3.79
16	4.45	5.93	4.89	5.53	5.93	7.75	6.68	7.20	6.10	5.14	5.28
17	6.04	7.72	6.46	6.76	7.72	9.28	8.35	8.82	7.83	6.98	6.96
18	7.68	9.57	8.08	8.03	9.57	10.85	10.08	10.48	9.62	8.88	8.70
19	9.26	11.36	9.65	9.25	11.36	12.37	11.74	12.09	11.34	10.71	10.38
20	10.65	12.94	11.03	10.33	12.94	13.71	13.20	13.51	12.85	12.32	11.85
21	11.94	14.40	12.32	11.33	14.40	14.96	14.56	14.82	14.26	13.82	13.23
22	13.13	15.76	13.52	12.25	15.76	16.11	15.82	16.04	15.55	15.20	14.50
23	14.22	17.01	14.62	13.10	17.01	17.17	16.96	17.16	16.73	16.46	15.66
24	15.22	18.14	15.64	13.87	18.14	18.14	18.01	18.18	17.81	17.61	16.72

5P											
QM	Outaouais	Chateaugu	Beauharnois	MIP	Assomption	Richelieu	Yamaska	St-Francois	Nicolet	DuLoup	Maskinongé
9	0.21	0.12	0.61	2.24	0.12	3.05	1.92	2.39	0.77	0.00	0.19
10	0.27	0.19	0.67	2.29	0.19	3.11	1.98	2.45	0.84	0.00	0.26
11	0.37	0.30	0.77	2.36	0.30	3.20	2.08	2.55	0.94	0.00	0.36
12	0.66	0.64	1.06	2.59	0.64	3.49	2.39	2.85	1.27	0.12	0.68
13	1.13	1.18	1.52	2.95	1.18	3.96	2.89	3.33	1.79	0.68	1.19
14	1.78	1.94	2.17	3.46	1.94	4.61	3.59	4.01	2.53	1.46	1.90
15	2.92	3.26	3.31	4.35	3.26	5.74	4.81	5.19	3.80	2.81	3.14
16	4.30	4.86	4.68	5.41	4.86	7.11	6.28	6.61	5.34	4.45	4.64
17	5.86	6.68	6.24	6.62	6.68	8.66	7.95	8.22	7.08	6.30	6.34
18	7.47	8.55	7.85	7.86	8.55	10.27	9.66	9.88	8.87	8.21	8.09
19	9.01	10.36	9.40	9.06	10.36	11.82	11.32	11.49	10.60	10.06	9.78
20	10.37	11.95	10.78	10.11	11.95	13.19	12.77	12.90	12.11	11.68	11.27
21	11.63	13.44	12.06	11.09	13.44	14.46	14.13	14.22	13.52	13.19	12.66
22	12.79	14.82	13.24	11.99	14.82	15.65	15.37	15.43	14.82	14.58	13.94
23	13.85	16.09	14.34	12.81	16.09	16.74	16.52	16.55	16.01	15.86	15.11
24	14.81	17.24	15.34	13.56	17.24	17.73	17.55	17.57	17.09	17.02	16.19

6P											
QM	Outaouais	Chateaugu	Beauharnois	MIP	Assomption	Richelieu	Yamaska	St-Francois	Nicolet	DuLoup	Maskinongé
9	0.26	0.00	0.52	2.28	0.00	3.72	1.43	1.77	0.40	0.00	0.00
10	0.31	0.00	0.58	2.32	0.00	3.77	1.49	1.83	0.46	0.00	0.00
11	0.40	0.00	0.68	2.39	0.00	3.87	1.59	1.93	0.57	0.00	0.00
12	0.68	0.00	0.97	2.61	0.00	4.17	1.90	2.23	0.89	0.00	0.00
13	1.13	0.00	1.43	2.95	0.00	4.64	2.40	2.71	1.42	0.27	0.22
14	1.75	0.69	2.08	3.43	0.69	5.30	3.10	3.38	2.15	1.06	0.95
15	2.82	2.04	3.21	4.27	2.04	6.45	4.31	4.56	3.43	2.43	2.20
16	4.12	3.67	4.58	5.28	3.67	7.84	5.78	5.98	4.97	4.09	3.73
17	5.59	5.52	6.14	6.41	5.52	9.42	7.43	7.59	6.72	5.97	5.45
18	7.09	7.43	7.74	7.57	7.43	11.06	9.14	9.25	8.52	7.91	7.24
19	8.53	9.29	9.30	8.69	9.29	12.64	10.79	10.85	10.25	9.79	8.96
20	9.79	10.92	10.66	9.67	10.92	14.04	12.23	12.26	11.77	11.44	10.48
21	10.95	12.45	11.94	10.56	12.45	15.35	13.57	13.57	13.19	12.98	11.89
22	12.01	13.87	13.12	11.39	13.87	16.56	14.81	14.79	14.49	14.40	13.21
23	12.97	15.17	14.22	12.13	15.17	17.68	15.95	15.90	15.69	15.70	14.41
24	13.84	16.37	15.21	12.80	16.37	18.70	16.98	16.92	16.77	16.89	15.52

7P											
QM	Outaouais	Chateaugu	Beauharnois	MIP	Assomption	Richelieu	Yamaska	St-Francois	Nicolet	DuLoup	Maskinongé
9	1.24	0.00	0.41	3.04	0.00	5.44	0.78	1.33	1.26	0.00	0.00
10	1.29	0.00	0.46	3.08	0.00	5.49	0.84	1.39	1.33	0.00	0.00
11	1.37	0.00	0.56	3.14	0.00	5.58	0.94	1.49	1.44	0.00	0.00
12	1.63	0.00	0.85	3.34	0.00	5.83	1.25	1.79	1.76	0.00	0.00
13	2.03	0.00	1.31	3.66	0.00	6.24	1.75	2.27	2.29	0.32	0.11
14	2.60	0.58	1.96	4.09	0.58	6.82	2.44	2.94	3.03	1.11	0.84
15	3.58	1.95	3.09	4.85	1.95	7.82	3.64	4.11	4.31	2.49	2.10
16	4.76	3.61	4.46	5.77	3.61	9.04	5.10	5.53	5.87	4.15	3.63
17	6.08	5.50	6.01	6.79	5.50	10.43	6.75	7.14	7.62	6.03	5.36
18	7.42	7.45	7.61	7.83	7.45	11.89	8.44	8.79	9.43	7.98	7.15
19	8.70	9.34	9.16	8.82	9.34	13.31	10.08	10.39	11.18	9.86	8.88
20	9.80	11.01	10.52	9.67	11.01	14.57	11.51	11.80	12.72	11.51	10.41
21	10.81	12.57	11.80	10.45	12.57	15.77	12.84	13.11	14.14	13.05	11.83
22	11.71	14.03	12.98	11.15	14.03	16.89	14.07	14.32	15.46	14.47	13.15
23	12.52	15.37	14.06	11.78	15.37	17.95	15.19	15.43	16.66	15.78	14.36
24	13.23	16.60	15.06	12.33	16.60	18.93	16.21	16.44	17.76	16.97	15.47

8P											
QM	Outaouais	Chateaugu	Beauharnois	MIP	Assomption	Richelieu	Yamaska	St-Francois	Nicolet	DuLoup	Maskinongé
9	3.05	0.00	0.25	2.43	0.00	5.90	0.44	1.23	6.11	0.00	0.00
10	3.09	0.00	0.30	2.47	0.00	5.95	0.50	1.29	6.17	0.00	0.00
11	3.17	0.00	0.40	2.55	0.00	6.04	0.60	1.39	6.28	0.00	0.00
12	3.40	0.00	0.69	2.76	0.00	6.29	0.91	1.68	6.61	0.00	0.00
13	3.77	0.00	1.15	3.11	0.00	6.70	1.41	2.17	7.14	0.47	0.09
14	4.29	0.73	1.80	3.60	0.73	7.27	2.10	2.84	7.89	1.26	0.82
15	5.19	2.11	2.92	4.46	2.11	8.28	3.30	4.01	9.18	2.64	2.08
16	6.26	3.78	4.29	5.50	3.78	9.50	4.75	5.43	10.75	4.31	3.61
17	7.45	5.67	5.83	6.69	5.67	10.89	6.39	7.03	12.52	6.20	5.35
18	8.65	7.63	7.43	7.93	7.63	12.34	8.08	8.68	14.35	8.15	7.14
19	9.78	9.54	8.97	9.15	9.54	13.76	9.71	10.28	16.11	10.03	8.87
20	10.74	11.22	10.33	10.23	11.22	15.03	11.13	11.68	17.66	11.69	10.40
21	11.61	12.79	11.60	11.26	12.79	16.22	12.46	12.99	19.11	13.23	11.82
22	12.38	14.26	12.78	12.23	14.26	17.35	13.68	14.20	20.44	14.66	13.14
23	13.05	15.61	13.86	13.14	15.61	18.40	14.80	15.31	21.66	15.98	14.36
24	13.62	16.85	14.85	13.98	16.85	19.38	15.81	16.32	22.78	17.18	15.47

Table 5: Accumulated degree-days for the “normal” climate, representing the interannual mean of QM, from 1953 to 2000 (number of degree °C over 5 °C).

Time in QM (quarter-month)	**Accumulated degree-days °C**
9	0.5
10	0.6
11	0.9
12	2.5
13	5.5

14	10.0
15	22.9
16	41.3
17	70.2
18	109.9
19	159.5
20	212.2
21	271.3
22	336.4
23	409.7
24	487.2

3.4. Calibration of diffusivity in the 2D temperature model

Lateral and longitudinal diffusion is the main factor controlling the temporal and spatial extent of a water masse within the river. In the model, it represents the impacts from turbulence and shear stress occurring in the river. This diffusivity is a nodal property that is derived from the hydrodynamic field; it can be controlled in the model by adjusting the "diffusivity coefficient". Calibration of this coefficient is a mandatory step for all transport-diffusion models.

In this study, we used temperature data calculated from remote sensing images for the calibration of the diffusivity coefficient. Remote sensing has the advantage of covering a large area instantaneously and gives a synthetic observation of the general temperature pattern of water masses. The thermal band (10.4-12.5 um) of Landsat-7 satellite was used to convert numerical values to surface water temperatures following a methodology from Bartoliucci and Chang (1988). The Landsat-7 image used for calibration was acquired on May 7th 2001. Prior to the calibration of diffusivity, hydrodynamic conditions of May 7th 2001 were simulated and were combined with meteorological data of QM 15 in the temperature model. These meteorological data were used because of their similarity with meteorological conditions of May 7th 2001. Water temperature of tributaries (boundary conditions) were determined using the *Banque de données sur la qualité du milieu aquatique* of the *Ministère de l'Environnement du Québec* which had available data on the same day for most tributaries of the St. Lawrence River. The result is a 2D simulation

of water temperatures that is used to calibrate the diffusion coefficient. The following section presents data produced with the final calibration.

3.4.1. Lake Saint-Louis calibration

The Figure 23 illustrates the results of a water temperature simulation and Landsat-7 image for the best calibration event. Note that the absolute values of water temperatures cannot be compared directly, simply because the Landsat-7 image was not calibrated with ground-truth data. Also, the Landsat-7 image gives the surface water temperature while the water temperature model gives the depth-averaged temperature. However, general patterns of water temperature mainly associated with different water masses can be compared. Generally, the model is able to reproduce the warmer conditions in shallow areas, especially in the Pointe-Claire Bay and at the south of Îles de la Paix. In this area, the model is able to reproduce the cold water coming from the south of Îles de la Paix. Also, the water temperature delimitation between the Ottawa River water and the Great Lakes river water is well reproduced by the model. There is an important difference in the general pattern in the north-eastern portion of the lake, which shows a relatively abrupt decline in water temperature that is not present in the model. We can not explain this situation; it might be associated with the presence of water vapour (faint clouds) in the area or an artefact of rapid cooling in the area the night before (not obvious in the hourly temperature data). This image is an instantaneous shot of the lake while the 2D model is considered to represent a steady state. No other images of the spring conditions were found because of the dense cloud cover during satellite passages over the area. However, we found an image from fall (November 11th, 1999) that shows an inverse situation in term of thermal pattern but with a very similar pattern in term of diffusion. Figure 24 shows a very similar pattern with the inverse thermal contrast, a typical situation for fall: warmer temperatures in the main water mass and cooler in shallower areas and in Ottawa River waters. Also notice the impact of topographical features like the ¸Îles de la Paix area or the shoals located in the central portion of the lake, north east of Île Perrot.

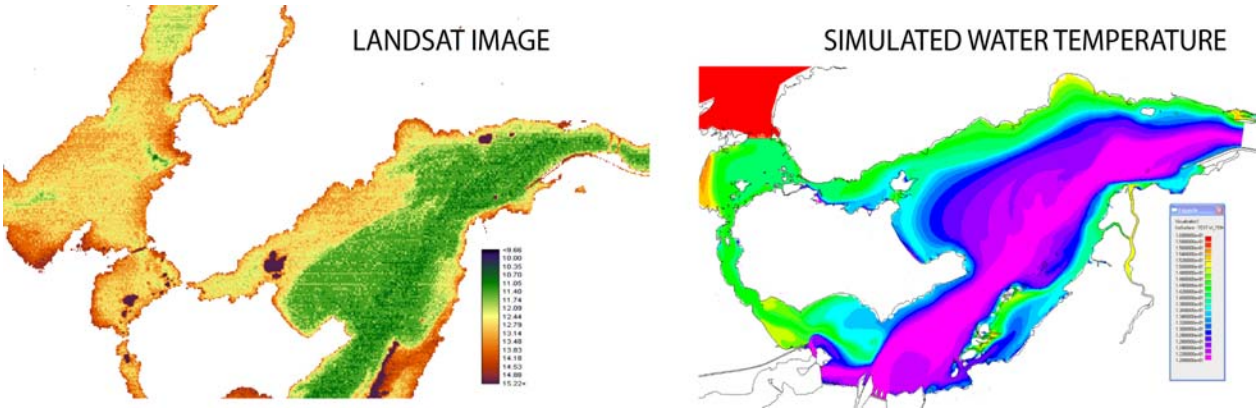

Figure 23: Calibration image showing the temperature description observed by Landsat-7 (May 7th, 2001) and the simulated conditions for the corresponding date in the Lake Saint-Louis area.

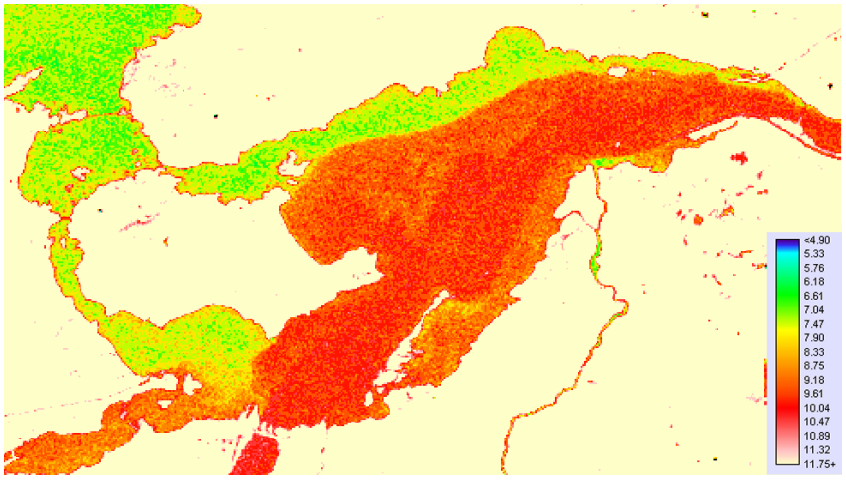

Figure 24: Landsat-7 image of Lake Saint-Louis area (November 11th, 1999), typical of the fall conditions and showing a water temperature pattern similar to simulated conditions.

3.4.2. Lake Saint-Pierre calibration

Figure 25 illustrates the results of a water temperature simulation compared to a Landsat-7 image for the calibration event. Overall, the water temperature model is able to reproduce the warmer temperatures in shallow areas, especially in the Saint-Francois Bay, Maskinongé Bay and on the south shore of Lake Saint-Pierre. Warmer temperatures in shallow areas within Sorel's Islands, like Île de Grâce and Grande Île are also well

reproduced. Spatial variations of water temperature patterns caused by the presence of islands and the impact of the main navigational channel in the center of the lake appear to be relatively well captured.

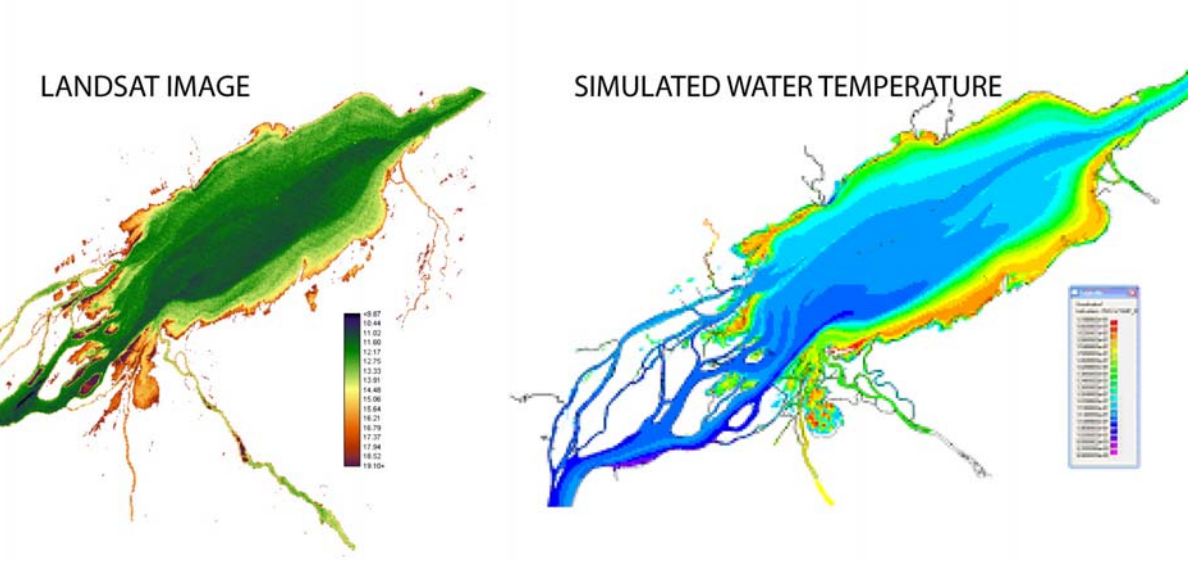

Figure 25: Calibration image showing the temperature description observed by Landsat-7 (May 7th 2001) and the simulated conditions for the corresponding date in the Lake Saint-Pierre area.

3.5. Lake Saint-Pierre water temperature during fish spawning periods

A total of 128 simulations of 2D water temperature were produced to cover the 16 QM and the 8 scenarios representing all possible hydraulic conditions. The following figure presents the results of simulations for the Lake Saint-Pierre area only. These simulations represent discharge events 4P to 6P, which are the most frequent during spring time. The simulated QM that are presented also represents the most frequent QM when fish spawning occurred (15 to 19).

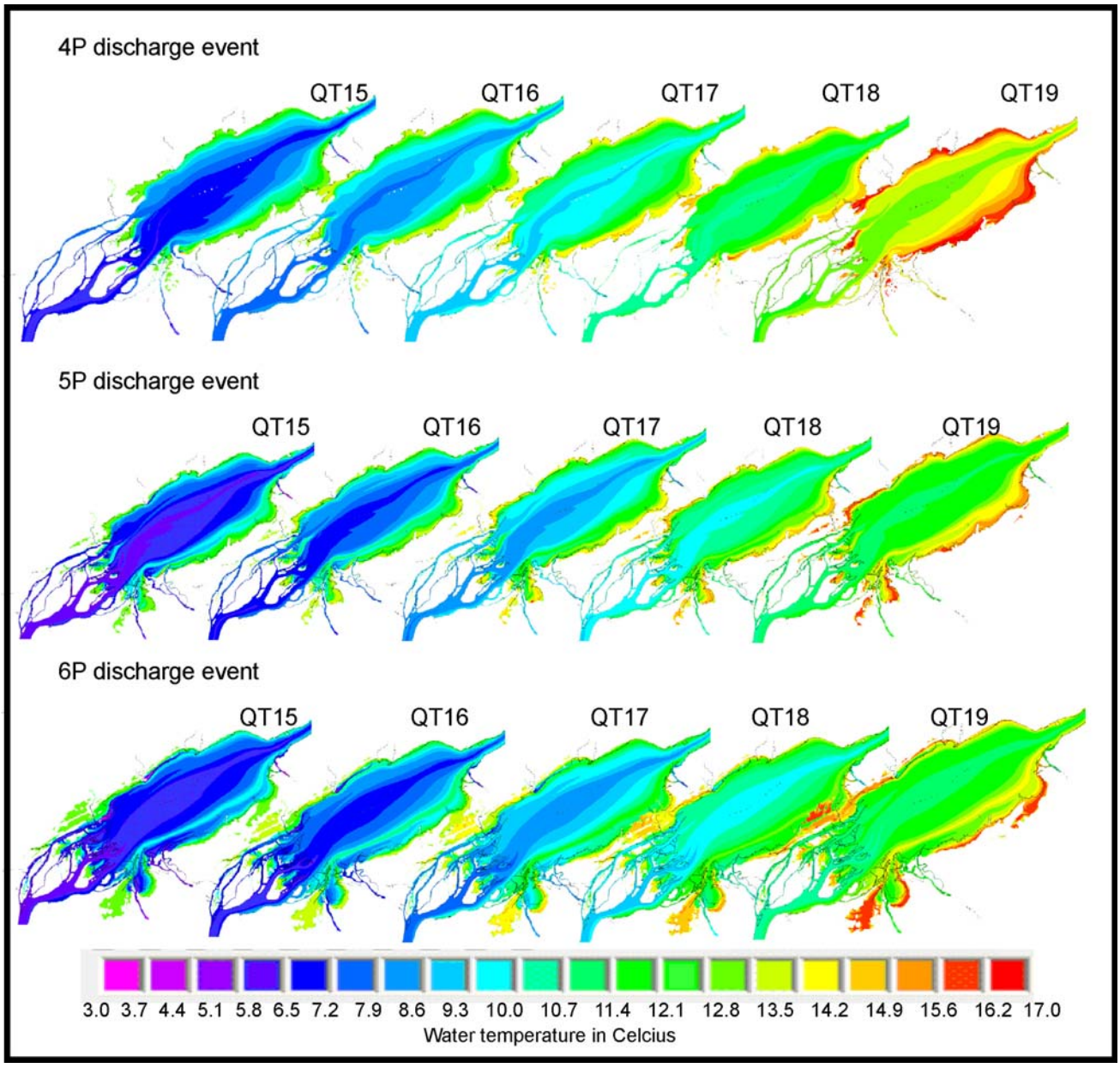

Figure 26: Simulated water temperature during the fish spawning period in the Lake Saint-Pierre area.

The images of Lake Saint-Pierre water temperature simulations show the temporal evolution (QM15 to QM19) of the water temperatures at a given discharge (4 to 6P). The figure can also be interpreted in the perpendicular direction which corresponds to the impact of either reduction or increase of discharge on the water temperatures. It can also be interpreted in the diagonal which allows the analysis of the combined change of

discharge and climatic parameters (or time based on the normal climate). It also fairly simple to understand that linear interpolation can be used to create any intermediate condition in term of climatic parameters and discharge, which is also true for all of the 128 simulations that cover the entire St. Lawrence River.

4. Conclusion

In order to fulfill the main objective of producing reliable 2D simulations of water temperatures for the entire St. Lawrence River for the spring time, we used hydrological analysis, a digital terrain model and hydrodynamic simulations produced prior to the present study. Calibration and validation of the 2D water temperature model has been performed with confident results in two other projects in the St. Lawrence River floodplain for spring time, and resulted in satisfactory prediction capabilities.

In this study, we have compiled and completed a series of relevant climatic parameters from 1953 to 2000 for Dorval station on a quarter-monthly (QM) mean. This series has been reduced for temperature modelling purposes into an interannual QM mean that was considered as the "normal" climate. Thus, normal climate has been used to drive the 2D temperature model and the corresponding values of accumulated degree-days were used for interpolation of any possible temperature conditions. Since 2D water temperature simulations were produced for fish spawning on the floodplain during early spring, we chose to reduce the number of simulations to a more efficient number of QM ranging from QM 9 to QM 24.

Boundary conditions for water temperatures of tributaries and inflows were derived from statistical temperature models specific to each tributary. Accumulated degree-days and tributary discharge were used in multivariate statistical models to predict the water temperatures at boundaries of the 2D water temperature model. The diffusion coefficient used in the 2D temperature model was calibrated using the thermal band from a Landsat-7 image and water temperature simulations for the same day as the Landsat-7 image. Using the normal climate as the driving variables and the tributaries boundary conditions, we have simulated 16 QM for 8 discharge scenarios for a total of 128 simulations of the entire St. Lawrence River.

References

Bartoliucci, L. A. and M. Chang (1988). Look-up Tables to Convert Landsat TM Thermal IR Data to Water Surface Temperatures. *Geocarto International*. **3**: 61-67.

Bouchard, A. and J. Morin (2000). Reconstitution des débits du fleuve Saint-Laurent entre 1932 et 1998. Environnement Canada, Service météorologique du Canada, Monitoring et Technologies, Section Hydrologie, Rapport Technique RT-101. 71 pages.

Fortin, R., P. Dumont, H. Fournier, C. Cadieux and D. Villeneuve (1982). Reproduction et force des classes d'âge du Grand Brochet (Esox lucius L.) dans le Haut-Richelieu et la baie Missisquoi. Can. J. Zool. **60**: 227-240.

Heniche, M., Y. Secretan, P. Boudreau and M. Leclerc (1999). A 2-D finite element drying-wetting shallow water model for rivers and estuaries. *Advances in Water Resources*. 35 pages.

Heniche, M., Y. Secretan, J. Morin, J.-F. Cantin and M. Leclerc (2002). Two-dimensional depth averaged fluvial thermal regime prediction. Submitted to *Journal of Hydraulic Engineering*.

Koonce, J. K., T. B. Bagenal, R. F. Carline, K. E. F. Hokanson and M. Nagiec (1977). Factors influencing year-class strength of Percids: A summary and a Model of temperature effects. *J. Fish. Res. Board Can*. **34**: 1900-1909.

Leclerc, M., A. Boudreault, J. Bechara and G. Corfa (1995). Two-dimensional hydrodynamic modelling: A neglected tool in the instream flow incremental methodology. *Transactions of the American Fisheries Society.* **124**: 645-662.

Morin, J., O. Champoux, A. Bouchard and D. Rioux (2003). High resolution 2D hydrodynamic modelling of Lake Saint-Louis: Definition of scenarios, simulation and validation/calibration. Rapport technique SMC Québec – Section Hydrologie RT-125. Environnement Canada, Sainte-Foy. 78 pages.

Morin, J., Y. Secretan, O. Champoux and A. Armellin (2002). Modélisation 2D de la température de l'eau sur la batture Tailhandier. Rapport technique SMC Québec – Section Hydrologie RT-117. Environnement Canada, Sainte-Foy. 71 pages.

Morin, J., Y. Secretan, O. Champoux et A. Armellin (2003). Modélisation 2D de la température de l'eau aux îles de Boucherville durant le printemps 2002. Rapport technique SMC Québec – Section Hydrologie RT-124. Environnement Canada, Sainte-Foy. 64 pages.

Secretan, Y., Y. Roy, Y. Granger et M. Leclerc (2000). MODELEUR/HYDROSIM – Guide d'utilisation. Document MODELEUR 1.0a07. Rapport INRS-Eau R482-G3F. 267p. p.v., Juin.

Wetzel, R. G. (2001). Limnology, lake and river ecosytems. Academic Press, Third edition. 106 pages.

Wootton, R. J. (1998). Ecology of Teleost fishes. Second edition. Kluwer Academic Publishers Fisn and Fisheries Series 24. 286 pages.